J. Fluid Mech. (1984), *vol.* 148, *pp.* 383–403
Printed in Great Britain

Longitudinal dispersion of matter due to the shear effect of steady and oscillatory currents

By HIDEKAZU YASUDA

Government Industrial Research Institute, Chugoku 15000, Hiromachi, Kure 737-01, Japan

(Received 2 September 1983 and in revised form 30 May 1984)

The longitudinal dispersion due to the shear effect of a current is examined theoretically in the idealized two-dimensional case. This study reveals the process whereby the dispersion reaches a stationary stage after the release of the dispersing substance as an instantaneous line source in steady and in oscillatory currents. In addition, the relation between the stationary dispersion coefficients in steady and oscillatory currents is given analytically. Analysis of the dispersion during the initial stage needs a clear definition of the vertical average of the variance. We can understand the problem of the negative dispersion coefficient, which is obtained by the usual vertical average, through introduction of a new vertical average.

1. Introduction

It has long been known that the 'shear effect', which is caused by the combined action of flow shear and mixing in the cross-sectional plane, has a strong influence on mass transport in pipes, channels, rivers, estuaries and inlets etc. Longitudinal dispersion due to the shear effect, after the great work of Taylor (1953, 1954), has been studied by many workers using theoretical analyses, hydraulic experiments, field observations and numerical analyses etc. (Fischer *et al.* 1979). Understanding the detailed nature of the shear effect from observing the actual dispersion of matter is difficult, because the shear effect is in reality a three-dimensional phenomenon. Thus most work on the shear effect has been concerned with theoretical analyses; although there has been a gap between the idealized models that have been used and the real phenomena, because of the assumptions made and the constraints imposed. Theoretical analyses are considered to be superior in understanding the basic nature of the phenomena insofar as there is not too much concern about numerical values. Many works on dispersion have used larger time periods and neglected periodic variation in the oscillatory current. The dispersion process from the initial to the stationary stage has scarcely been clarified analytically. Though Smith (1982) analysed the variance and the dispersion coefficient during the initial stage in the oscillatory current, he showed that the dispersion coefficient was sometimes negative. Smith (1983) also explained that the increasing rate of the variance (corresponding to the dispersion coefficient) at a particular level is negative in reversing flows of oscillatory currents. The negative dispersion coefficient is not considered to be reasonable if we regard the dispersion due to the shear effect as a kind of mixing phenomena such as turbulent diffusion.

Yasuda (1982) examined the dispersion structure due to the oscillatory boundary layer, with understanding of the behaviour at each level, and pointed out the problem of the vertical average of the dispersion coefficient. The present paper will study the dispersion process from the initial to the stationary stage in both steady and

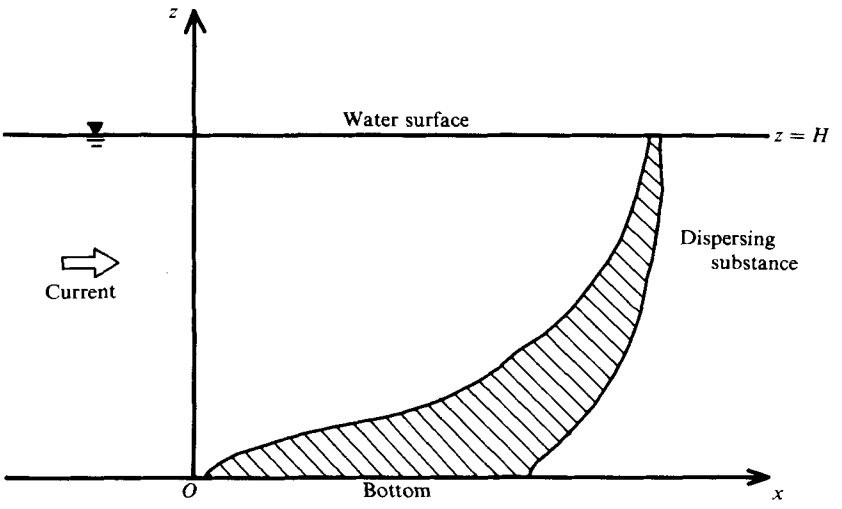

FIGURE 1. Two-dimensional model of dispersion due to shear effect. The dispersing substance is released as an instantaneous line source at $x = 0$.

oscillatory currents with typical vertical profile, in which a new definition of the vertical average of the dispersion will be proposed. It will clarify the nature of the dispersion due to the shear effect and the problem of the negative dispersion coefficient.

2. Analysis of the advective–diffusion equation in the two-dimensional plane

This study will analyse the longitudinal dispersion due to the shear effect in the two-dimensional (x, z)-plane, neglecting the variation with y (figure 1). If the current $u(z, t)$, independent of x, flows along the x-axis, the advective–diffusion equation governing the concentration of the diffusing substance $S(x, z, t)$ can be written as

$$\frac{\partial S}{\partial t} + u(z,t)\frac{\partial S}{\partial x} = k_x \frac{\partial^2 S}{\partial x^2} + k_z \frac{\partial^2 S}{\partial z^2}, \tag{1}$$

where t is time, and k_x and k_z are diffusion coefficients (assumed constant). In order to make the theoretical considerations easier, the water depth is assumed constant, and the diffusing substance is completely passive, as can be seen from (1). The boundary conditions for $S(x, z, t)$ are

$$\left.\begin{aligned} &\frac{\partial S}{\partial z} = 0 \quad \text{at } z = 0 \text{ (bottom) and } z = H \text{ (water surface)}, \\ &S = 0 \quad \text{as } x \to \pm\infty. \end{aligned}\right\} \tag{2}$$

The initial condition is

$$S(x, z, 0) = \frac{S_0}{H}\delta(x), \tag{3}$$

where S_0 represents the total amount of the diffusing substance and $\delta(x)$ is the Dirac delta function. The initial condition (3) corresponds to an instantaneous line source at $x = 0$ due to the absence of variation with y-direction. When the current $u(z, t)$ is independent of x, Aris's (1956) method of moments can apply for analysis of the

matter dispersion. Knowledge of the various moments of the material concentration suggests the behaviour of the concentration distribution. The pth-order moment of the concentration at level z and time t is defined as

$$M_p(z,t) = \int_{-\infty}^{\infty} x^p S(x,z,t)\,\mathrm{d}x, \tag{4}$$

where p can take any positive integer value. The equation governing the pth-order moment is given by (1) and (2) as

$$\frac{\partial M_p}{\partial t} - k_z \frac{\partial^2 M_p}{\partial z^2} = puM_{p-1} + p(p-1)\kappa_x M_{p-2}, \tag{5}$$

with the boundary condition

$$\frac{\partial M_p}{\partial z} = 0 \quad \text{at } z = 0 \text{ and } z = H. \tag{6}$$

$M_0(z,t)$ means the amount of the dispersing material at level z, and the normalized pth-order moment is given by

$$\mu_p(z,t) = \frac{M_p(z,t)}{M_0(z,t)}. \tag{7}$$

Furthermore the normalized and central pth-order moment can be defined as

$$\phi_p(z,t) = \frac{1}{M_0(z,t)} \int_{-\infty}^{\infty} (x-\mu_1)^p S(x,z,t)\,\mathrm{d}x. \tag{8}$$

The variance at level z is

$$\sigma_x^2(z,t) = \phi_2(z,t) = \mu_2 - \mu_1^2. \tag{9}$$

The skewness factor and the flatness factor are

$$\mathscr{S}(z,t) = \frac{\phi_3}{\sigma_x^3}, \qquad \mathscr{F}(z,t) = \frac{\phi_4}{\sigma_x^4} - 3, \tag{10),(11}$$

where σ_x is the standard deviation. The longitudinal dispersion coefficient at level z and time t is defined in terms of $\sigma_x^2(z,t)$ as

$$D(z,t) = \frac{1}{2} \frac{\mathrm{d}\sigma_x^2(z,t)}{\mathrm{d}t}. \tag{12}$$

The dispersion coefficient $D(z,t)$, which indicates the degree of the dispersion effect, is obtained from the zeroth-, the first- and the second-order moments. Though the skewness factor and the flatness factor, obtained from the third- and the fourth-order moments, are regarded as important during the initial stage of matter dispersion, the present study does not solve these higher-order moments, since the emphasis is on the dispersion coefficient. Equations governing the zeroth-, the first- and the second-order moments are written as follows:

$$\frac{\partial M_0}{\partial t} - k_z \frac{\partial^2 M_0}{\partial z^2} = 0, \tag{13}$$

$$\frac{\partial M_1}{\partial t} - k_z \frac{\partial^2 M_1}{\partial z^2} = uM_0, \tag{14}$$

$$\frac{\partial M_2}{\partial t} - k_z \frac{\partial^2 M_2}{\partial z^2} = 2uM_1 + 2kxM_0. \tag{15}$$

Boundary conditions for various moments are given in (6). The initial condition for the zeroth order moment is $M_0 = S_0/H$ $(t = 0)$, and those for the other various moments are $M_p = 0$ $(t = 0)$. Let the current $u(z, t)$ be expressed as

$$u(z,t) = U \sum_{i=1}^{k} \zeta_i(z)\,\eta_i(t), \tag{16}$$

where ζ_i and η_i are functions of z and t respectively. The meaning of (16) is as follows: it is a steady flow if $k = 1$ and $\eta_1 = 1$, a transient flow if $k = 1$ and $\eta_1 = 1-\mathrm{e}^{-t}$, and an oscillatory flow without phase lag if $k = 1$ and $\eta_1 = \sin\omega t$(or $\cos\omega t$). Furthermore, Yasuda's (1982) analysis corresponds to the case in which $k = 2$, $\zeta_1 = 1-\mathrm{e}^{-\beta z}\cos\beta z$, $\zeta_2 = \mathrm{e}^{-\beta z}\sin\beta z$, $\eta_1 = \sin\omega t$ and $\eta_2 = \cos\omega t$, where ω is frequency of the oscillation and β is a constant determined by frequency and viscosity.

The solution of the zeroth-order moment is invariant with time in the case of an instantaneous line source. Therefore

$$M_0(z,t) = \frac{S_0}{H}. \tag{17}$$

Equations (14) and (15) are non-homogeneous heat-conduction equations, as is well known. If the right-hand side of each equation is known, we can obtain a formal solution (Yasuda 1982). The formal expression for the first-order moment is given as

$$M_1(z,t) = \frac{S_0}{H}\mu_1(z,t) = \frac{S_0}{H}\left[\frac{U}{H}\sum_{n=0}^{\infty}\epsilon_n\left\{\sum_{i=1}^{k}\int_0^H \zeta_i(\xi)\cos\frac{n\pi}{H}\xi\,\mathrm{d}\xi\int_0^t \mathrm{e}^{\chi_n\tau}\eta_i(\tau)\,\mathrm{d}\tau\right\}\mathrm{e}^{-\chi_n t}\cos\frac{n\pi}{H}z\right]. \tag{18}$$

If we put

$$\int_0^H \zeta_i(\xi)\cos\frac{n\pi}{H}\xi\,\mathrm{d}\xi = \alpha_{ni}(H), \qquad \int_0^t \mathrm{e}^{\chi_n\tau}\eta_i(\tau)\,\mathrm{d}\tau = \beta_{ni}(t)$$

then the second-order moment is expressed as

$$M_2(z,t) = \frac{S_0}{H}\mu_2(z,t) = \frac{S_0}{H}\left[2k_x t + 2\frac{U^2}{H^2}\sum_{n=0}^{\infty}\epsilon_n\left\{\sum_{m=0}^{\infty}\epsilon_m\sum_{i=1}^{k}\sum_{j=1}^{k}\alpha_{mi}(H)\right.\right.$$
$$\left.\left.\times\int_0^H \zeta_j(\xi)\cos\frac{m\pi}{H}\xi\cos\frac{n\pi}{H}\xi\,\mathrm{d}\xi\int_0^t \mathrm{e}^{(\chi_n-\chi_m)\tau}\beta_{mi}(\tau)\,\eta_j(\tau)\,\mathrm{d}\tau\right\}\mathrm{e}^{-\chi_n t}\cos\frac{n\pi}{H}z\right], \tag{19}$$

where $\epsilon_n = \{1(n = 0), 2(n \neq 0)\}$ and $\chi_n = (n\pi)^2 k_z/H^2$. The right-hand side of (19) can be seen to consist of two independent terms: one due to the horizontal diffusivity and the other due to the combined action of flow shear and vertical diffusivity. Because the horizontal diffusivity has no effect on the flow shear in this model, we neglect the horizontal-diffusion effect and pay attention only to the above combined action in the following discussion. Substituting a reasonable functional formula for the current profile into (18) and (19), we can obtain the analytical behaviour of the dispersion in the steady, oscillatory and the other time-dependent flows.

3. Vertically averaged solutions of the equations governing the dispersion due to the shear effect

Yasuda (1982) analysed the vertical profile of the variance in the oscillatory current forming the oscillatory boundary layer (sometimes called the 'Stokes boundary layer'). Principally, this study will take notice of the vertically averaged values, which

have been worked on generally by many researchers. There are two methods of taking the average of the variance as follows:

$$\bar{\sigma}_x^2(t) = \bar{\phi}_2(t) = \bar{\mu}_2 - \overline{\mu_1^2}, \tag{20}$$

$$\bar{\sigma}_x^2(t)^* = \frac{1}{\bar{M}_0}\int_{-\infty}^{\infty} (x-\bar{\mu}_1)^2\,\bar{S}(x,t)\,\mathrm{d}x = \bar{\mu}_2 - \overline{\mu_1^2}. \tag{21}$$

The overbar denotes the vertical average. Equation (20) gives the averaged variance in the vertical direction and gives the degree of mixing. On the other hand, (21) is obtained from averaging the concentration of the diffusing substance and contains the degree of stretching by flow shear besides that of mixing. Though there is little difference between both variances when t is large and the dispersing substance is well-mixed vertically, it is necessary to pay attention to this distinction especially during the initial stage. From (20) and (21) we can define the respective vertically averaged dispersion coefficients as follows:

$$\bar{D}(t) = \frac{1}{2}\frac{\mathrm{d}\bar{\sigma}_x^2}{\mathrm{d}t}, \qquad \bar{D}(t)^* = \frac{1}{2}\frac{\mathrm{d}\bar{\sigma}_x^{2*}}{\mathrm{d}t}. \tag{22),(23}$$

The vertical averages of the first- and second-order moments and so on are obtained as

$$\bar{\mu}_1 = \frac{U}{H}\alpha_{01}(H)\,\beta_{01}(t), \tag{24}$$

$$\begin{aligned}\overline{\mu_1^2} &= \frac{U^2}{H^2}\left[\alpha_{01}^2(H)\,\beta_{01}^2(t) + 2\sum_{m=1}^{\infty}\alpha_{m_1}^2(H)\,\beta_{m_1}^2(t)\,\mathrm{e}^{-2\chi_m t}\right]\\ &= \overline{\mu_1^2} + \frac{U^2}{H^2}\left[2\sum_{m=1}^{\infty}\alpha_{m_1}^2(H)\,\beta_{m_1}^2(t)\,\mathrm{e}^{-2\chi_m t}\right],\end{aligned} \tag{25}$$

$$\bar{\mu}_2 = 2\frac{U^2}{H^2}\left[\sum_{m=0}^{\infty}\epsilon_m\,\alpha_{m_1}(H)\,A_{m0_1}(H)\,B_{m0_{11}}(t)\right], \tag{26}$$

where

$$A_{mn_1}(H) = \int_0^H \zeta_1(\xi)\cos\frac{m\pi}{H}\xi\,\cos\frac{n\pi}{H}\xi\,\mathrm{d}\xi, \quad B_{mn_{11}}(t) = \int_0^t \mathrm{e}^{(\chi_n-\chi_m)\tau}\beta_{m_1}(\tau)\,\eta_1(\tau)\,\mathrm{d}\tau.$$

Substitution of (24)–(26) into (20) and (21) yields

$$\overline{\sigma_x^2} = \frac{U^2}{H^2}\left[4\sum_{m=1}^{\infty}\alpha_{m_1}(H)\,A_{m0_1}(H)\,B_{m0_{11}}(t) - 2\sum_{m=1}^{\infty}\alpha_{m_1}^2(H)\,\beta_{m_1}^2(t)\,\mathrm{e}^{-2\chi_m t}\right], \tag{27}$$

$$\overline{\sigma_x^2}^* = \frac{U^2}{H_2}\left[4\sum_{m=1}^{\infty}\alpha_{m_1}(H)\,A_{m0_1}(H)\,B_{m0_{11}}(t)\right]. \tag{28}$$

If $\alpha_{m_1}(H)$, $\beta_{m_1}(t)$, $A_{mn_1}(H)$ and $B_{mn_{11}}(t)$ can be integrated, the dispersion coefficient is expressed analytically.

In order to analyse the longitudinal dispersion, this study adopts the following two kinds of vertical profile of the current (figure 2):

$$(a)\quad \zeta_1(z) = \begin{cases}1 & (d \leqq z \leqq H),\\ 0 & (0 \leqq z \leqq d),\end{cases} \tag{29}$$

$$(b)\quad \zeta_1(z) = \begin{cases}1 & (d \leqq z \leqq H),\\ \dfrac{z}{d} & (0 \leqq z \leqq d).\end{cases} \tag{30}$$

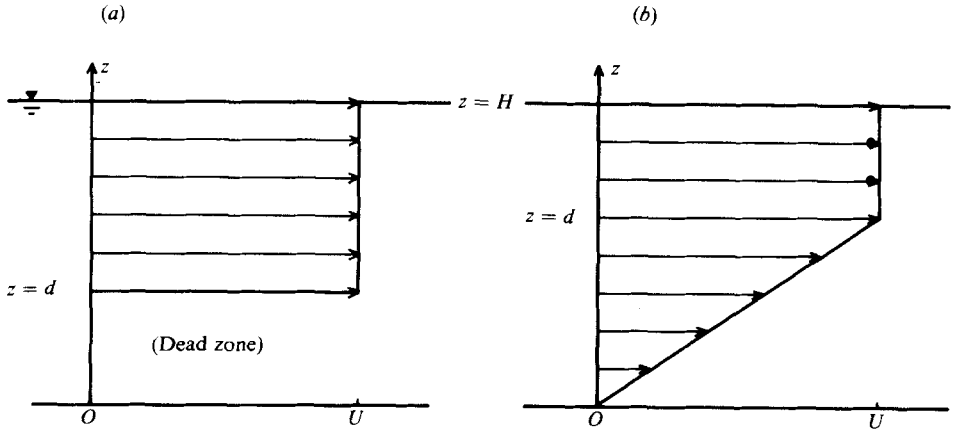

FIGURE 2. Vertical profiles of the current in this study: (*a*) the two-layer flow; (*b*) the linear flow.

(*a*) is a two-layer flow, and the region of $0 \leqq z \leqq d$ is called the 'dead zone of flow'. When $d = H$ in (*b*), it is a well-known Couette flow having constant shear throughout the depth. The value of d is arbitrary from 0 to H in both profiles. The profiles (*a*) and (*b*) are respectively called the 'two-layer flow' and the 'linear flow' in the following discussion. The oscillatory current in this study will neglect the effect of the phase distribution for simplicity, i.e. $k = 1$ and $\eta_1 = \sin \omega t$.

3.1. *Analytical solutions in the case of the steady current*

By substituting velocity profiles as mentioned above into (22)–(28), we can represent the vertically averaged variance etc. as follows:

$$\bar{\mu}_1 = UT_c[a_0 t^*], \tag{31}$$

$$\bar{\mu}_2 = U^2T_c^2\left[a_0^2 t^{*2} + \sum_{m=1}^{\infty} a_m \left\{t^* - \frac{1-\mathrm{e}^{-(m\pi)^2 t^*}}{(m\pi)^2}\right\}\right], \tag{32}$$

$$\bar{\sigma}_x^2 = U^2T_c^2\left[\sum_{m=1}^{\infty} a_m \left\{t^* - \frac{1}{2(m\pi)^2}\langle 1-\mathrm{e}^{-(m\pi)^2 t^*}\rangle \langle 3-\mathrm{e}^{-(m\pi)^2 t^*}\rangle\right\}\right], \tag{33}$$

$$\bar{\sigma}_x^{2*} = U^2T_c^2\left[\sum_{m=1}^{\infty} a_m \left\{t^* - \frac{1-\mathrm{e}^{-(m\pi)^2 t^*}}{(m\pi)^2}\right\}\right], \tag{34}$$

$$\bar{D} = U^2T_c\left[\sum_{m=1}^{\infty} \frac{a_m}{2}\{1-\mathrm{e}^{-(m\pi)^2 t^*}\}^2\right]. \tag{35}$$

$$\bar{D}^* = U^2T_c\left[\sum_{m=1}^{\infty} \frac{a_m}{2}\{1-\mathrm{e}^{-(m\pi)^2 t^*}\}\right], \tag{36}$$

where $t^* = t/T_c$, and $T_c = H^2/k_z$ is called the characteristic time of vertical mixing. a_0 and a_m are expressed as

$$a_0 = \begin{cases} 1-d^* & \text{for the two-layer flow } (a), \\ 1-\frac{1}{2}d^* & \text{for the linear flow } (b), \end{cases} \tag{37}$$

$$a_m = \begin{cases} \dfrac{4}{(m\pi)^4}\sin^2 m\pi d^* & \text{for } (a), \\ \dfrac{4}{(m\pi)^6}\dfrac{(\cos m\pi d^* - 1)^2}{d^{*2}} & \text{for } (b), \end{cases} \tag{38}$$

where $d^* = d/H$. When t is large as $e^{-\pi^2 t^*}$ tends to zero, the dispersion coefficient becomes steady. The steady dispersion coefficients are written as

$$\bar{D}_s = \bar{D}_s^* = U^2 T_c \sum_{m=1}^{\infty} \tfrac{1}{2} a_m. \tag{39}$$

Suffix s denotes the steady state. If higher-order terms of a_m are negligibly small, the vertically averaged dispersion coefficients are approximated as

$$\bar{D} = U^2 T_c [\tfrac{1}{2} a_1 \{1 - e^{-\pi^2 t^*}\}^2], \tag{40}$$

$$\bar{D}^* = U^2 T_c [\tfrac{1}{2} a_1 \{1 - e^{-\pi^2 t^*}\}]. \tag{41}$$

The steady coefficients in this condition are expressed as

$$\bar{D}_s = \bar{D}_s^* = \tfrac{1}{2} U^2 T_c a_1. \tag{42}$$

Substitution of $d^* = 1$ into (38) yields $a_1 = 1/60.0868...$ in the case of a linear flow. This almost completely corresponds to Bowden's (1965) analysis, where $\bar{D}_s = \frac{1}{120} U^2 T_c$ in the case of a linear flow with constant shear in all depth.†

3.2. *Analytical solutions in the case of an oscillatory current*

The vertically averaged variance etc. in the case of an oscillatory current with $k = 1$ and $\eta_1 = \sin \omega t$ are expressed analytically as follows:

$$\bar{\mu}_1 = U T_c [a_0 T_0(t^*)], \tag{43}$$

$$\bar{\mu}_2 = U^2 T_c^2 \left[a_0^2 T_0^2(t^*) + \sum_{m=1}^{\infty} a_m E_m(T_r) T_m(t^*) \right], \tag{44}$$

$$\bar{\sigma}_x^2 = U^2 T_c^2 \left[\sum_{m=1}^{\infty} a_m E_m(T_r) T_{vm}(t^*) \right], \tag{45}$$

$$\bar{\sigma}_x^{2*} = U^2 T_c^2 \left[\sum_{m=1}^{\infty} a_m E_m(T_r) T_m(t^*) \right], \tag{46}$$

$$\bar{D} = U^2 T_c \left[\sum_{m=1}^{\infty} \tfrac{1}{2} a_m E_m(T_r) T'_{vm}(t^*) \right], \tag{47}$$

$$\bar{D}^* = U^2 T_c \left[\sum_{m=1}^{\infty} \tfrac{1}{2} a_m E_m(T_r) T'_m(t^*) \right], \tag{48}$$

where

$$T_0(t^*) = \frac{1 - \cos 2\pi T_r t^*}{2\pi T_r},$$

$$T_m(t^*) = \tfrac{1}{2}(m\pi)^2 t^* + \frac{2\pi T_r}{(m\pi)^4 + (2\pi T_r)^2} [2\pi T_r - e^{-(m\pi)^2 t^*} \{(m\pi)^2 \sin 2\pi T_r t^* + 2\pi T_r \cos 2\pi T_r t^*\}] - \frac{1}{4} \left\{ 1 - \cos 4\pi T_r t^* + \frac{(m\pi)^2}{2\pi T_r} \sin 4\pi T_r t^* \right\},$$

$$T_{vm}(t^*) = \tfrac{1}{2}(m\pi)^2 t^* + \frac{1}{(m\pi)^4 + (2\pi T_r)^2} [(2\pi T_r)^2 \{1 - \tfrac{1}{2} e^{-2(m\pi)^2 t^*}\} - 4\pi T_r (m\pi)^2 e^{-(m\pi)^2 t^*} \sin 2\pi T_r t^* + \tfrac{1}{4} \langle \{(m\pi)^2 - (2\pi T_r)^2\} \cos 4\pi T_r t^* + 4\pi T_r (m\pi)^2 \sin 4\pi T_r t^* \rangle - \tfrac{1}{4}] - \tfrac{1}{4} \left\{ 1 - \cos 4\pi T_r t^* + \frac{(m\pi)^2}{2\pi T_r} \sin 4\pi T_r t^* \right\},$$

† The characteristic velocity U_b is the vertical averaged value in Bowden's (1965) analysis. Though $\bar{D}_s = \frac{1}{30} U_b^2 T_c$ was given in his work, it corresponds to $\bar{D}_s = \frac{1}{120} U^2 T_c$ in the present paper.

$$T'_m(t^*) = \tfrac{1}{2}(m\pi)^2 + 2\pi T_r\, e^{-(m\pi)^2 t^*} \sin 2\pi T_r t^* - \{\pi T_r \sin 4\pi T_r t^* + \tfrac{1}{2}(m\pi)^2 \cos 4\pi T_r t^*\},$$

$$\begin{aligned} T'_{vm}(t^*) = {} & \tfrac{1}{2}(m\pi)^2 + \frac{2\pi T_r}{(m\pi)^4 + (2\pi T_r)^2} \langle 2\pi T_r (m\pi)^2 e^{-2(m\pi)^2 t^*} \\ & + 2(m\pi)^2 e^{-(m\pi)^2 t^*} \{(m\pi)^2 \sin 2\pi T_r t^* \\ & - 2\pi T_r \cos 2\pi T_r t^*\} + 2\pi T_r (m\pi)^2 \cos 4\pi T_r t^* - \tfrac{1}{2}[(m\pi)^4 - (2\pi T_r)^2] \sin 4\pi T_r t^* \rangle \\ & - \{\pi T_r \sin 4\pi T_r t^* + \tfrac{1}{2}(m\pi)^2 \cos 4\pi T_r t^*\}, \end{aligned}$$

$$E_m(T_r) = \frac{(m\pi)^2}{(m\pi)^4 + (2\pi T_r)^2}, \quad T_r = \frac{T_c}{T}.$$

a_0 and a_m are the same as those in the steady current. Though the dispersion coefficients (47) and (48) are seemingly complicated, we can express them in a simplified form at large values of time as $e^{-\pi^2 t^*}$ tends to zero.

$$\begin{aligned} \bar{D}_{t\to\infty} = U^2 T_c \sum_{m=1}^{\infty} \tfrac{1}{2} a_m E_m(T_r) \Big[\tfrac{1}{2}(m\pi)^2 - \Big\langle \pi T_r \Big\{ 1 + \frac{(m\pi)^4 - (2\pi T_r)^2}{(m\pi)^4 + (2\pi T_r)^2} \Big\} \sin 4\pi T_r t^* \\ + \tfrac{1}{2}(m\pi)^2 \Big\{ 1 - \frac{2(2\pi T_r)^2}{(m\pi)^4 + (2\pi T_r)^2} \Big\} \cos 4\pi T_r t^* \Big\rangle \Big] \end{aligned} \tag{49}$$

$$\bar{D}^*_{t\to\infty} = U^2 T_c \sum_{m=1}^{\infty} \tfrac{1}{2} a_m E_m(T_r) [\tfrac{1}{2}(m\pi)^2 - \langle \pi T_r \sin 4\pi T_r t^* + \tfrac{1}{2}(m\pi)^2 \cos 4\pi T_r t^* \rangle]. \tag{50}$$

The argument $2\pi T_r t^*$ of each trigonometrical function corresponds to ωt (ω is the frequency of the oscillatory current). Thus it is recognized from (47)–(50) that, though the dispersion coefficient has cyclical variations with the same frequency as the oscillatory current during the initial stage, it fluctuates with only a double frequency at large t. The dispersion coefficient in the oscillatory current changes cyclically with a double-frequency period infinitely, though that in the steady current reaches a steady and constant value as time proceeds. In order to understand the long-term variation, we often disregard the variation with the frequency of the oscillatory current. The vertically averaged variances at every tidal period, which is given by substituting $\cos 2\pi T_r t^* = \cos 4\pi T_r t^* = 1$ and $\sin 2\pi T_r t^* = \sin 4\pi T_r t^* = 0$, are written as follows:

$$\bar{\sigma}^2_{x\mathrm{M}} = U^2 T_c^2 \sum_{m=1}^{\infty} a_m E_m(T_r) \Big[\tfrac{1}{2}(m\pi)^2 t^* + \frac{(2\pi T_r)^2}{(m\pi)^4 + (2\pi T_r)^2} \frac{1 - e^{-2(m\pi)^2 t^*}}{2} \Big], \tag{51}$$

$$\bar{\sigma}^{2*}_{x\mathrm{M}} = U^2 T_c^2 \sum_{m=1}^{\infty} a_m E_m(T_r) \Big[\tfrac{1}{2}(m\pi)^2 t^* + \frac{(2\pi T_r)^2}{(m\pi)^4 + (2\pi T_r)^2} \{1 - e^{-(m\pi)^2 t^*}\} \Big]. \tag{52}$$

The tidally averaged dispersion coefficients at each tidal period are given by the difference between the above variance at the $(l+1)$th tidal period and that at the lth one:

$$\begin{aligned} \bar{D}_{\mathrm{M}} = U^2 T_c \sum_{m=1}^{\infty} \tfrac{1}{2} a_m E_m(T_r) \Big[\tfrac{1}{2}(m\pi)^2 + \frac{(2\pi T_r)^2}{2\{(m\pi)^4 + (2\pi T_r)^2\}} \\ \times \exp\Big[-\frac{2(m\pi)^2}{T_r} l \Big] \Big\{ 1 - \exp\Big[-\frac{2(m\pi)^2}{T_r} \Big] \Big\} \Big], \end{aligned} \tag{53}$$

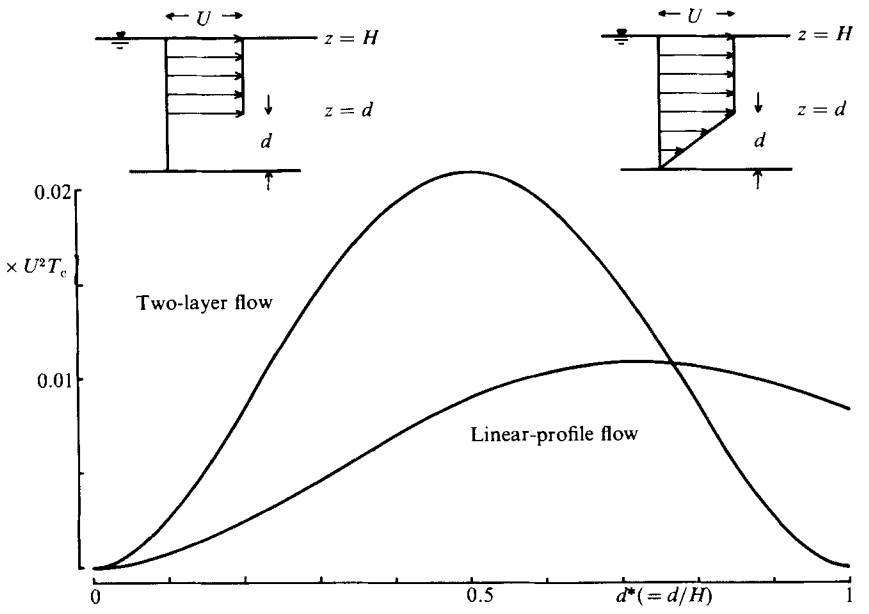

FIGURE 3. Stationary dispersion coefficients in the steady current for each d^*.

$$\bar{D}^*_{\mathrm{M}} = U^2 T_{\mathrm{c}} \sum_{m=1}^{\infty} \tfrac{1}{2} a_m E_m(T_{\mathrm{r}}) \left[\tfrac{1}{2}(m\pi)^2 + \frac{(2\pi T_{\mathrm{r}})^2}{(m\pi)^4 + (2\pi T_{\mathrm{r}})^2} \times \exp\left[-\frac{(m\pi)^2}{T_{\mathrm{r}}} l \right] \left\{ 1 - \exp\left[-\frac{2(m\pi)^2}{T_{\mathrm{r}}} \right] \right\} \right], \quad (54)$$

where l is any positive integer. The steady values at large l are

$$\bar{D}_{\mathrm{s}} = \bar{D}^*_{\mathrm{s}} = U^2 T_{\mathrm{c}} \sum_{m=1}^{\infty} \frac{a_m}{4} \frac{(m\pi)^4}{(m\pi)^4 + (2\pi T_{\mathrm{r}})^2} = U^2 T_{\mathrm{c}} \sum_{m=1}^{\infty} \tfrac{1}{4} a_m (m\pi)^2 E_m(T_{\mathrm{r}}). \quad (55)$$

If T_{r} is very small the dispersion coefficient in the oscillatory current is half of that in the steady current, as shown by Bowden (1965).

4. Solution curves of the vertically averaged dispersion

From the analysis in §3 we can recognize that the stationary dispersion coefficient in the steady current of (39) is the most basic one. Figure 3 illustrates it with each d^* (from zero to unity) in both typical current profiles. The dispersion coefficient has a maximum at $d^* = 0.5$ in the case of the two-layer flow, as is to be expected. Though it is considered to have a maximum at $d^* = 1$ in the case of the linear flow, unexpectedly it reaches a maximum at $d^* = 0.72$.

The dispersion coefficient in the oscillatory current is recognized to depend on the value of T_{r}($= T_{\mathrm{c}}/T$) from (55). This is shown in figure 4 for the case of each flow profile. The case $d^* = 1$ in the linear flow corresponds to Couette flow, and the curve for this case is identical with that of Holly, Harleman & Fischer (1970). This figure shows that the rate of decrease of the dispersion coefficient to T_{r} varies for each flow profile.

Figure 5 represents the variation of the vertically averaged variance with time in the steady flow with $d^* = 0.5$ of the two-layer flow. Figure 6 shows the variation of

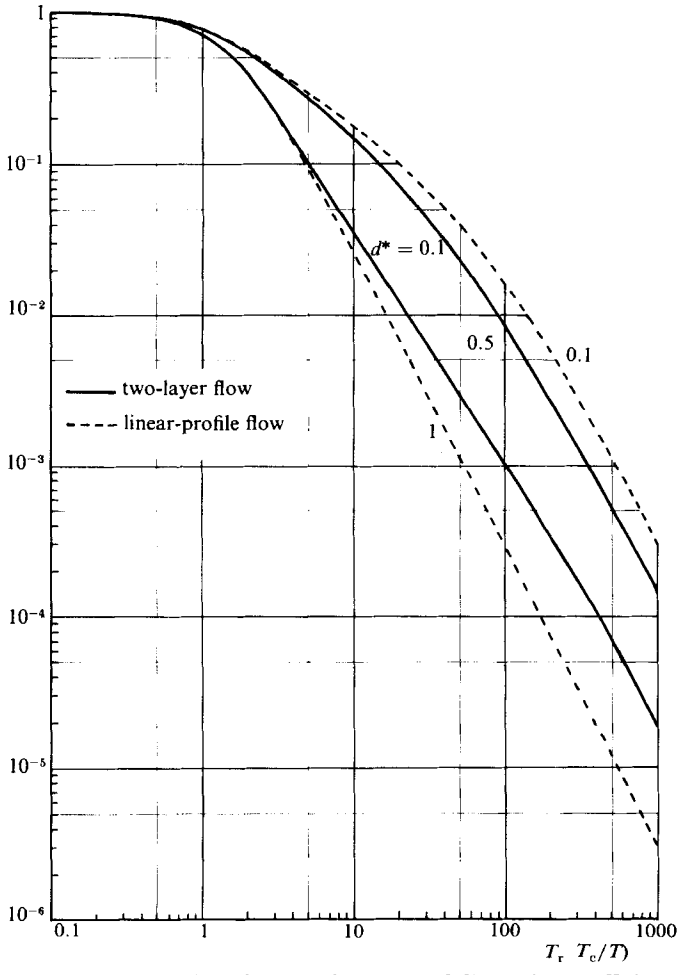

FIGURE 4. Variations with $T_r (= T_c/T)$ of one-cycle-averaged dispersion coefficients at the stationary state for a few typical velocity profiles. The dispersion coefficients of the ordinate are normalized by those for very small T_r.

the vertically averaged dispersion coefficient with time. The dispersion coefficient can be seen to reach steady state when the time approaches nearly a half of the characteristic time T_c of vertical mixing. This figure indicates that $\overline{D}^*$ is larger than $\overline{D}$ during the transient state until steady. Such processes of the variation of the dispersion coefficient with time are almost similar to one another, even if the current profiles are different. Figure 7 shows the variation of the variance with time in the oscillatory current ($\eta_1 = \sin \omega t$), the vertical profile of which is identical with that of figure 5. Figure 8 shows the dispersion coefficient corresponding to figure 7. The equation $\eta_1 = \sin \omega t$ means that a line source is released at the slack period, which is shown by a thick solid line. A thin solid line in these figures illustrates the case of $\eta_1 = \cos \omega t$, which means that a line source is released at the maximum flow period. Figures 7 and 8 are for the case $T_r = 10$. The dispersion coefficient reaches the stationary state in both the steady current and the oscillatory one when $e^{-\pi^2 t^*}$ tends to zero. Therefore the stationary state approximates to the period of $t^* \geqq 0.5$. Though approaching a constant value in the steady current as time proceeds, the dispersion

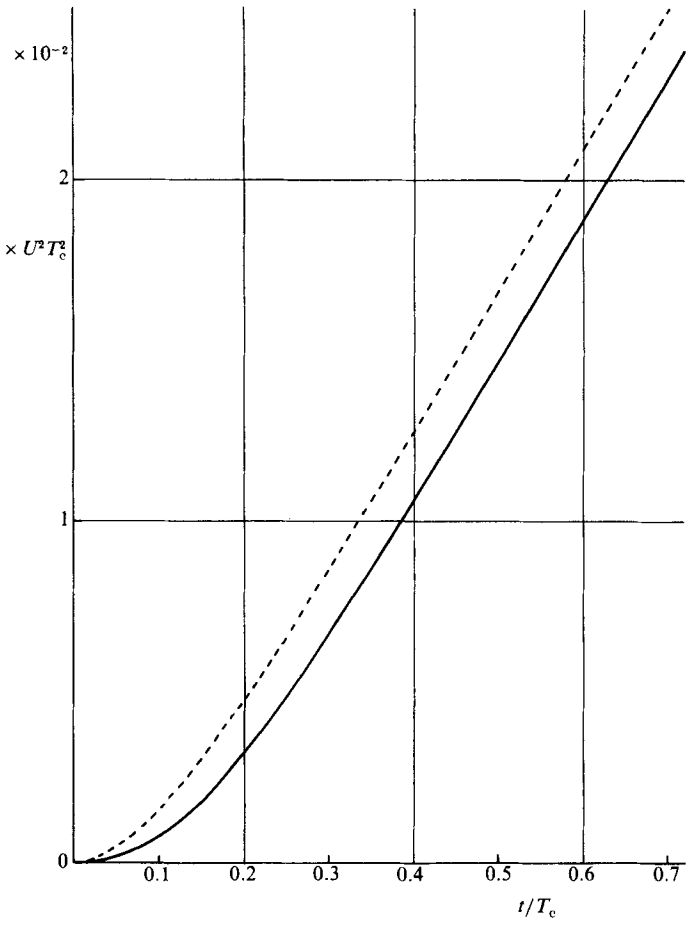

FIGURE 5. Temporal changes of the vertically averaged variances in the steady current with two-layer profile ($d^* = 0.5$) as given by (33) and (34), which correspond respectively to a solid line and a broken line.

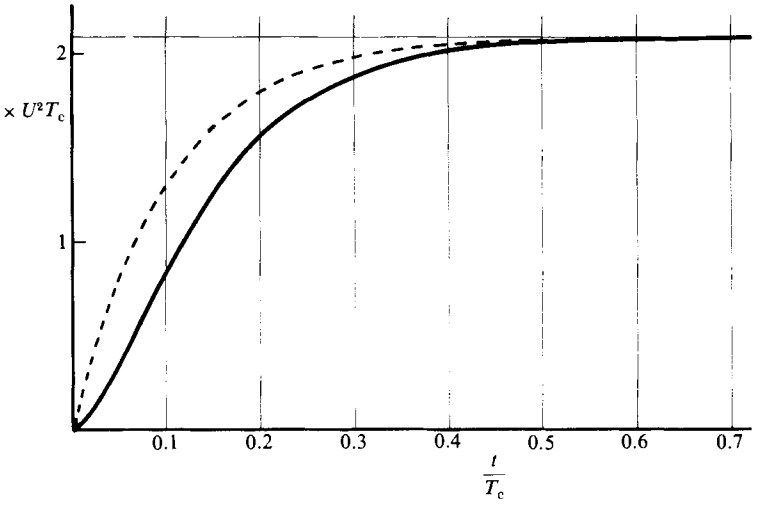

FIGURE 6. The dispersion coefficients with the same current as in the case of figure 5 given by (35) (solid line) and (36) (broken line).

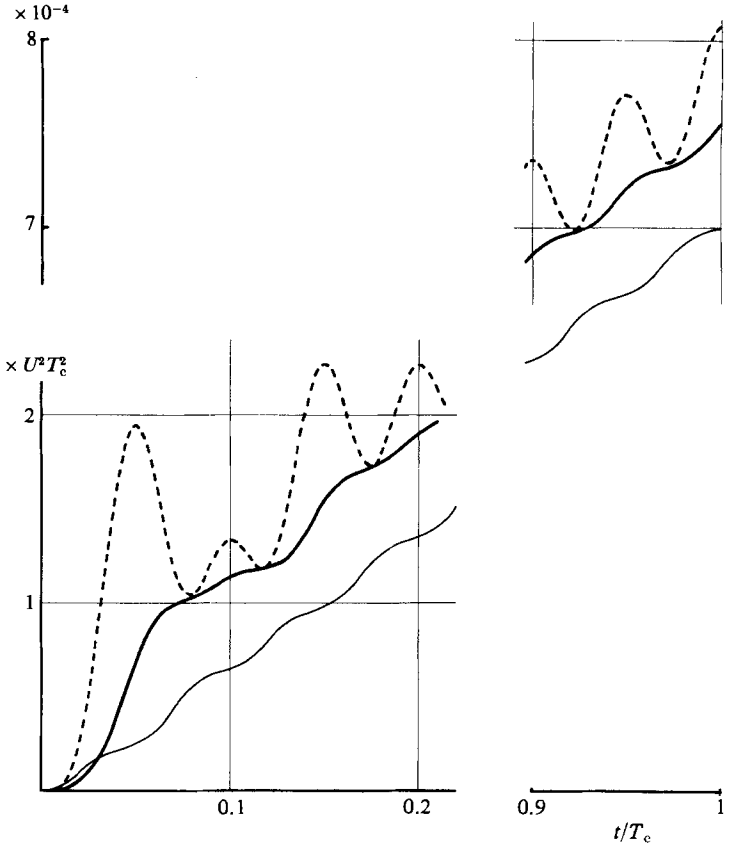

FIGURE 7. The variations of the vertical averaged variance with time in the oscillatory current with two-layer profile ($d^* = 0.5$). The thick solid and broken lines correspond to (45) and (46) respectively. The thin solid line is for $\eta_1 = \cos\omega t$, which means that a line source is released at the maximum flow period. ($T_r = 10.$)

coefficient changes cyclically in the oscillatory current even in the stationary state, as is expected from the results of §3. The dispersion coefficient $\bar{D}^*$, obtained by the averaging method of previous researchers, is sometimes negative. This results from increase and decrease of the shear of the first-order moment, and the detailed structure will be illustrated in §5. The dispersion coefficient $\bar{D}$, proposed in the present study and representing the degree of mixture of the substance, is by no means negative, even when it is very small. Figures 9 and 10 show variances and dispersion coefficients when $T_r = 100$ with the same current profile as figures 7 and 8. When T_r is large, which results from small k_z, the two types of vertically averaged dispersion coefficient are very different from one another. Figures 11 and 12 show variances and dispersion coefficients for the case $T_r = 10$ with $d^* = 1$ of the linear flow. Figure 13 is the variation with each tidal period of the dispersion coefficient in the case $d^* = 0.5$ of the two-layer-flow. The vertically averaged dispersion coefficient without cyclical change can be seen to reach the steady value more rapidly than the period that $e^{-\pi^2 t^*}$ becomes nearly zero, especially when T_r is large.

5. Vertical structure of shear diffusion

Though the dispersion coefficient is generally evaluated through the vertical (or cross-sectional) average, the study of the variation of its vertical profile with time is considered to help us to understand better the nature of the dispersion due to the

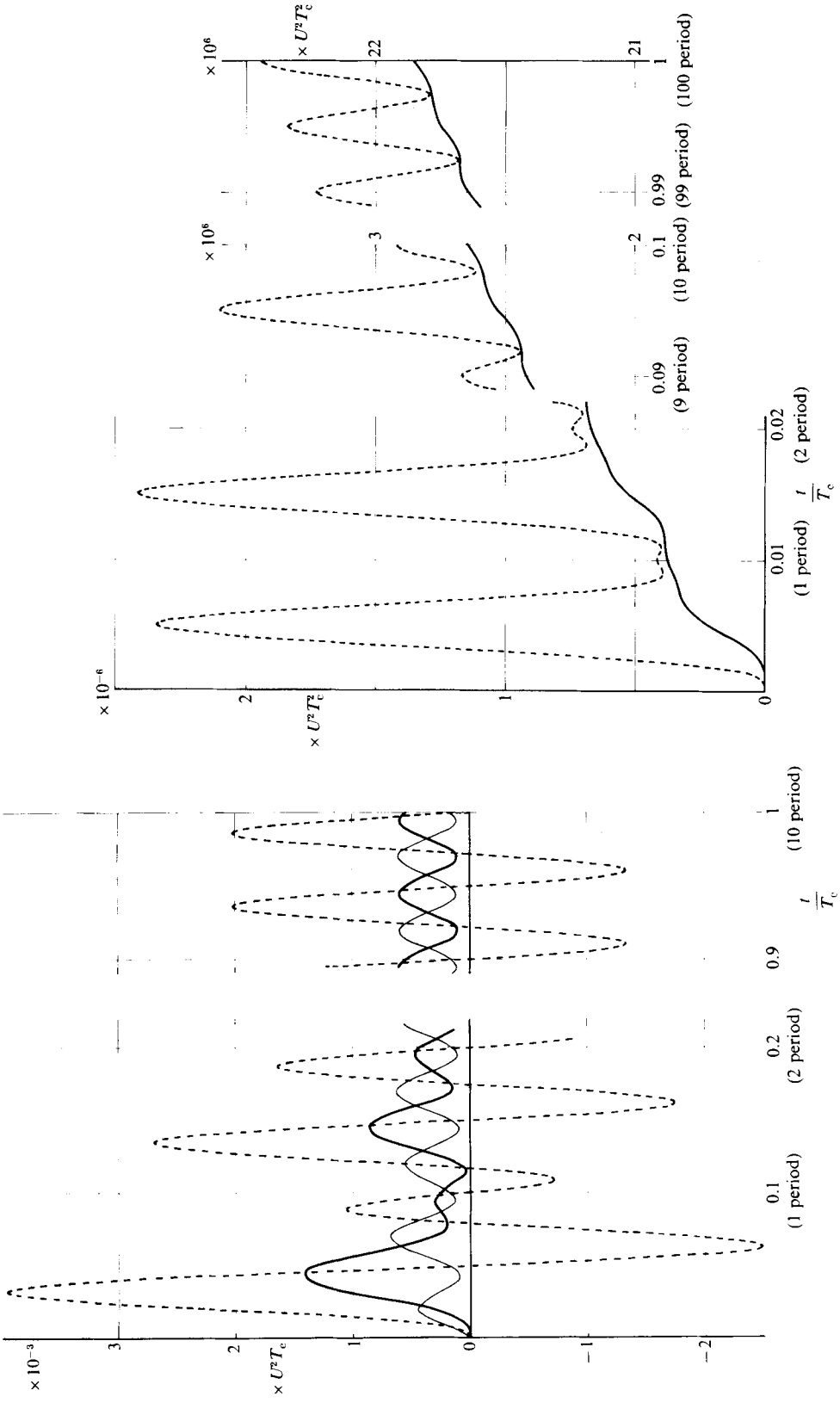

FIG. 8

FIGURE 8. The dispersion coefficients with the same conditions as figure 7. The thick solid line and the broken line correspond to (47) and (48) respectively. The thin solid line is for $\eta_1 = \cos \omega t$.

FIGURE 9. The variances in the case $T_r = 100$. The current profile is identical with that of figure 7.

FIG. 9

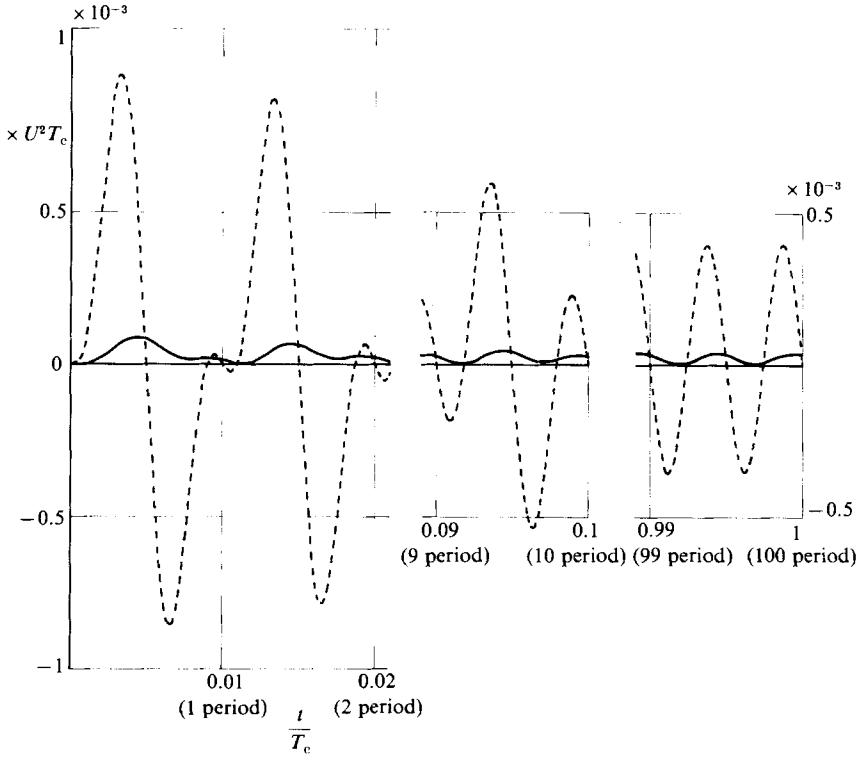

FIGURE 10. The dispersion coefficients with the same condition as figure 9.

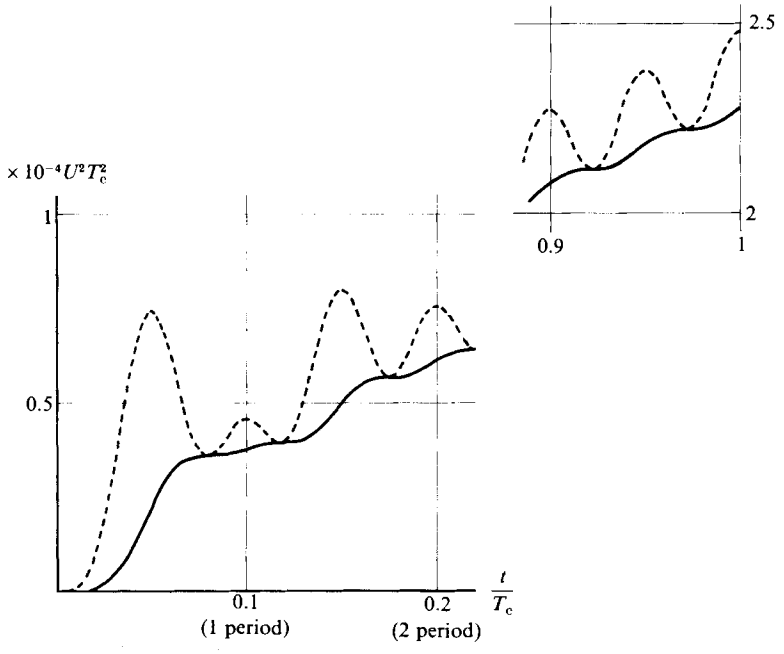

FIGURE 11. The variances in the oscillatory current with linear profile ($d^* = 1$ and $T_r = 10$).

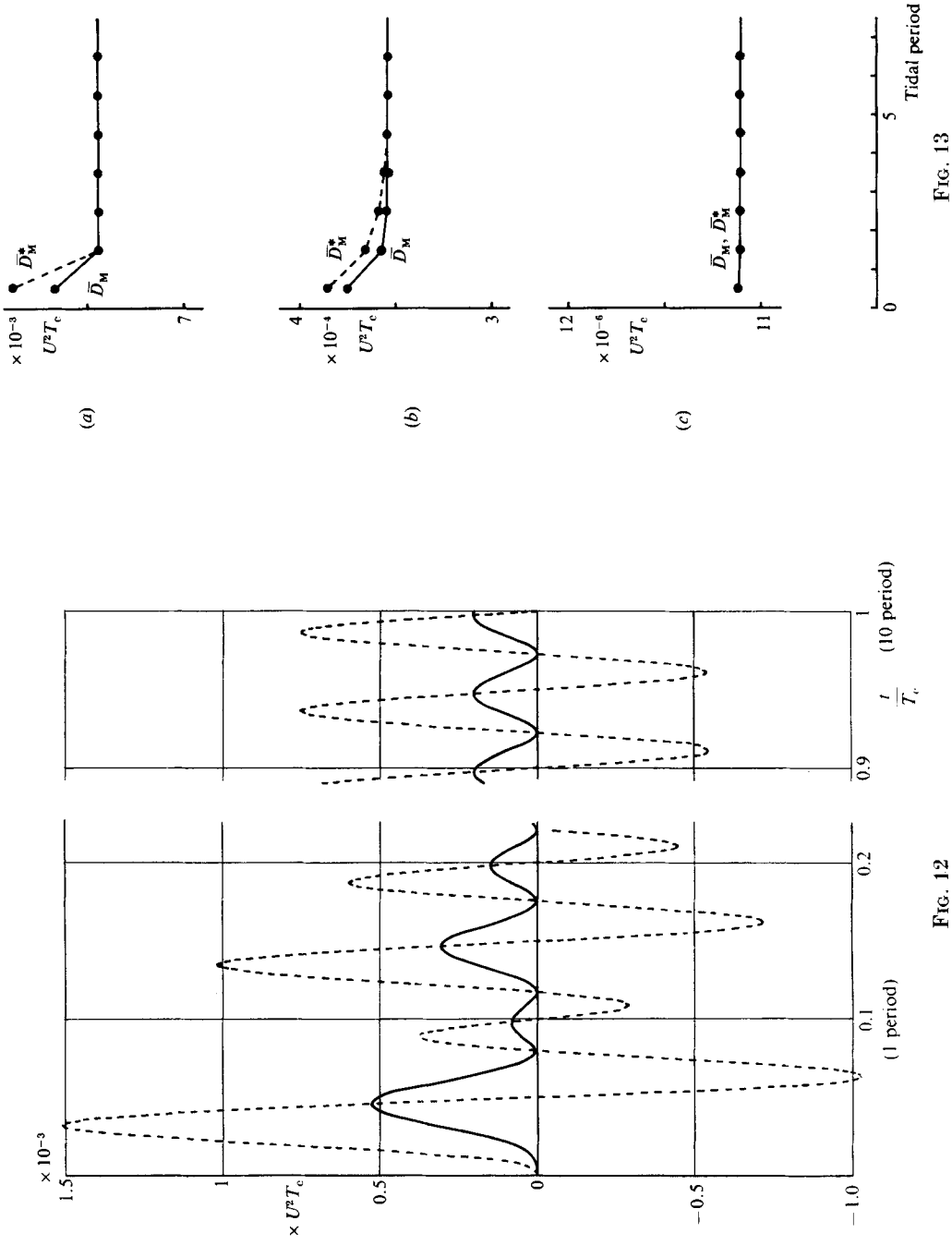

FIG. 12

FIGURE 12. The dispersion coefficients with the same condition as figure 11.

FIGURE 13. Variations of the dispersion coefficients with each tidal period in the case $d^* = 0.5$ of the two-layer flow as given by (53). (*a*), (*b*) and (*c*) are respectively the cases $T_r = 1$, 10 and 100.

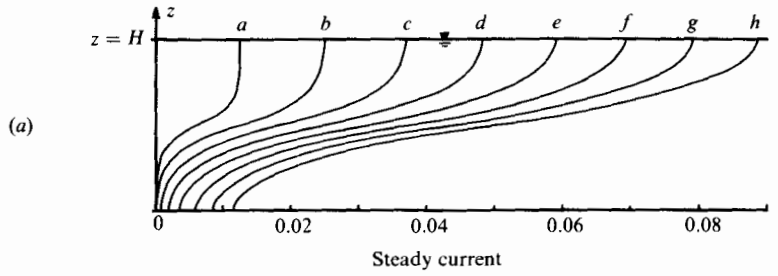

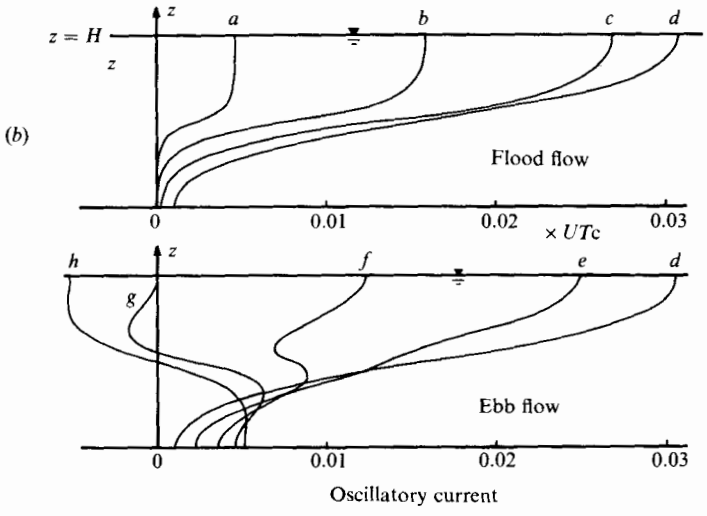

FIG. 14

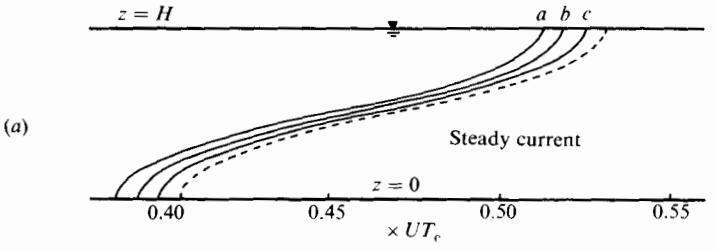

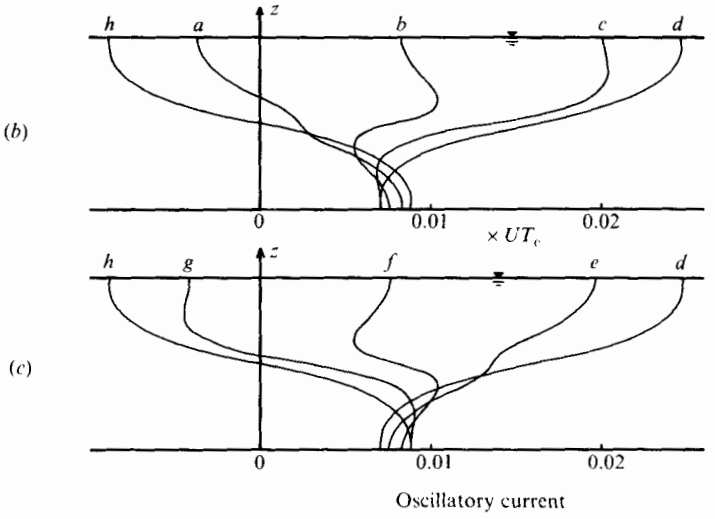

FIG.15

FIGURE 14. Temporal changes of the vertical profile of the first-order moment during the initial stage. The current is the case $d^* = 0.5$ of the two-layer profile, and the time interval is $\frac{1}{80}T_c$. (*a*) The steady current; (*b*) the oscillatory current for $T_r = 10$.

FIGURE 15. The first-order moment during the stationary stage $t^* \geqq 0.9$: (*a*) the steady current; (*b*) the oscillatory current for $T_r = 10$.

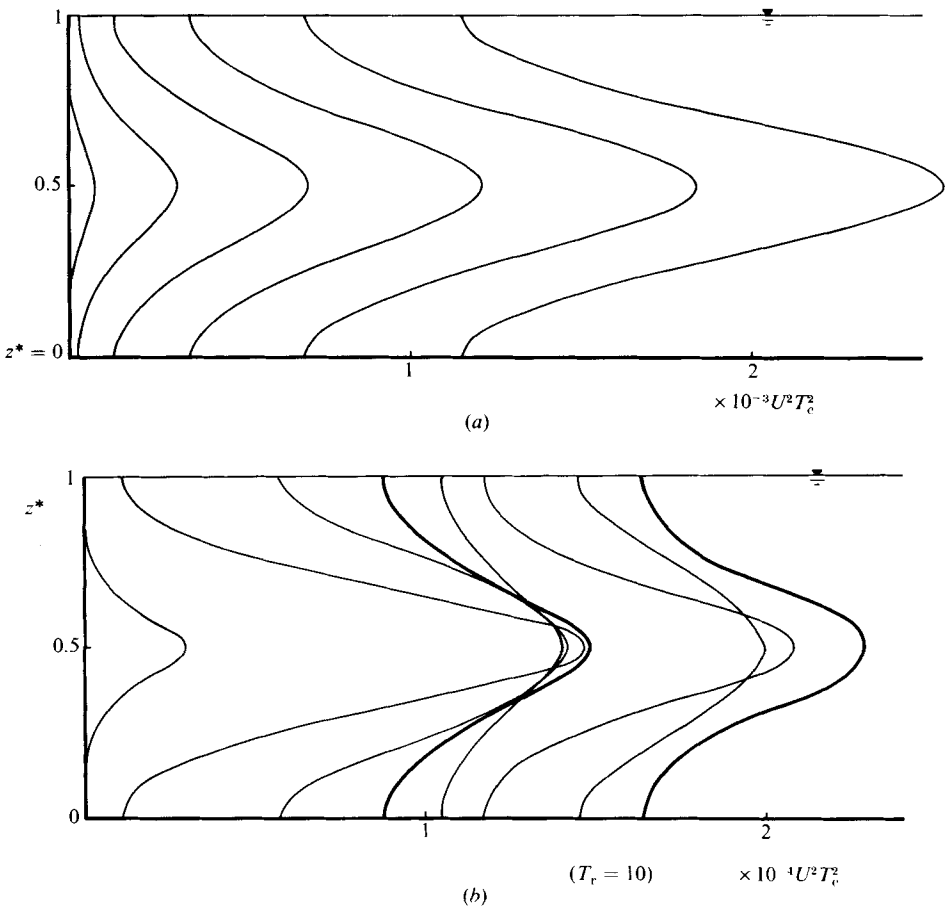

FIGURE 16. The variations of the vertical profile of the variance with time ($d^* = 0.5$ of the two-layer flow): (*a*) the steady current; (*b*) the oscillatory current for $T_r = 10$.

shear effect. This section will show a few examples of the vertical structure of the dispersion.

The vertical structures of the variance and the dispersion coefficient etc. can be found by substitution of (18) and (19) into (9) and (12) etc. In figure 14 is shown the temporal change of the vertical profile of the first-order moment during the initial stage. Figures 14 (*a*) and (*b*) are the cases of the steady and the oscillatory currents respectively. The current profile is $d^* = 0.5$ for two-layer flow and $T_r = 10$ in the case of the oscillatory current. Figure 15 shows during the stationary stage ($t^* = 0.9 \sim 1$). The time interval of each profile in both figures is $\frac{1}{80}T_c$. In the oscillatory current one tidal period corresponds to $\frac{1}{10}T_c$, where $T_r = 10$. We can see from figure 15 that the dispersion coefficient can have a variation with double frequency in the oscillatory current, since the vertical profiles of the first-order moment for the flood period is completely symmetric with those for the ebb period. Figure 16 illustrates the temporal change of the vertical profile of the variance with the same current condition as that of figure 14. This figure explains that the dispersion is at first generated at the level $z^* = d^*$ (where a difference in velocity appears, or in other words the flow shear is maximum) and gradually transmitted in the vertical direction. Figure 17

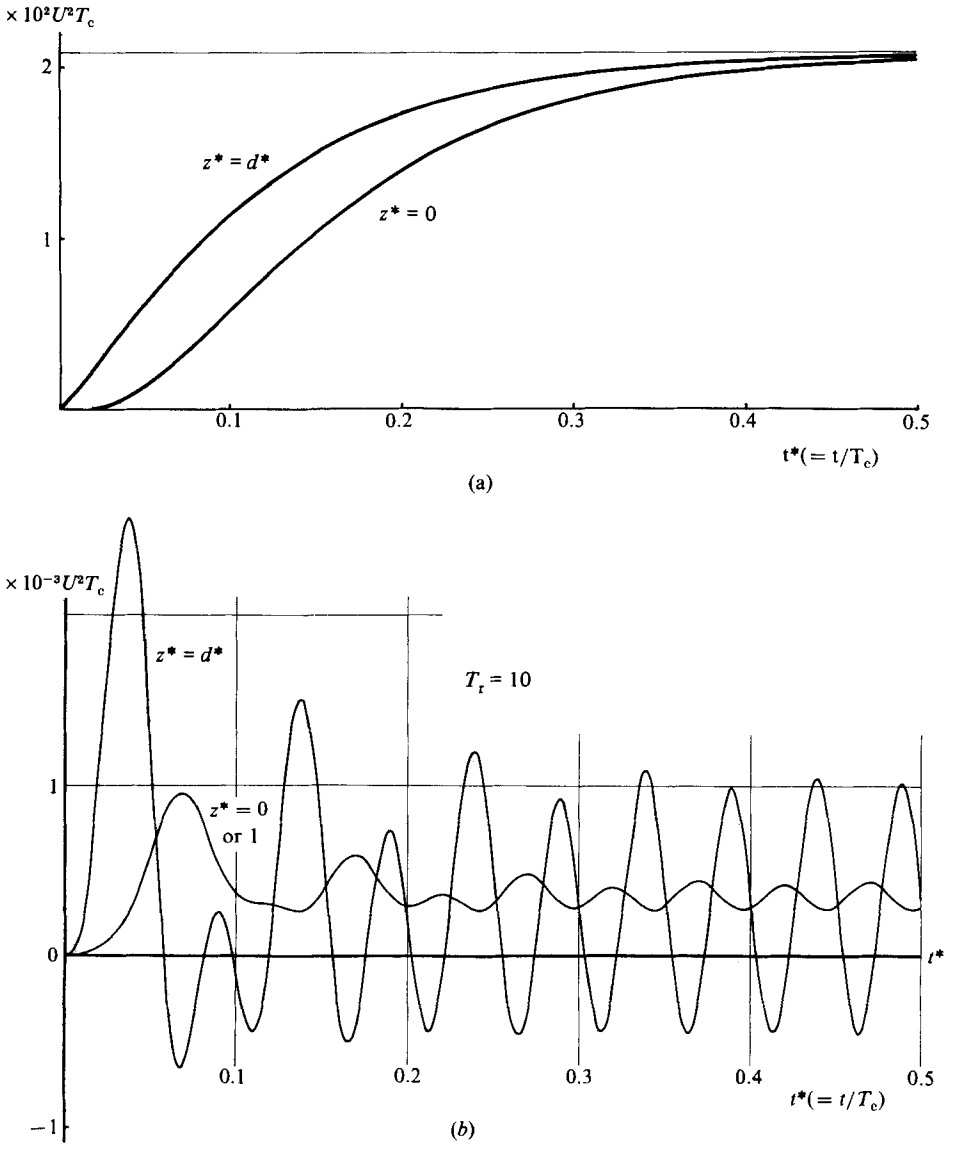

FIGURE 17. Temporal changes of the dispersion coefficient at $z^* = d^*$ and at $z^* = 0$ or 1 ($d^* = 0.5$ of the two-layer flow): (*a*) the steady current; (*b*) the oscillatory current for $T_r = 10$.

shows the variations of the dispersion coefficient with time at $z^* = 0.5$ (where the velocity gap appears) and $z^* = 0$ or 1 (bottom or water surface). Note that the dispersion coefficient at level z can be rewritten from (14), (15) and (12) as†

$$D(z,t) = \frac{k_z}{2}\left(\frac{\partial^2 \mu_2}{\partial z^2} - 2\mu_1 \frac{\partial \mu_1}{\partial z}\right). \tag{56}$$

Although the dispersion coefficients at two typical levels reach the same constant value with time in the steady current, they fluctuate separately in the oscillatory current, even at large time.

† Since μ_2 and μ_1 are formally expressed as $\Sigma_{n=0}^{\infty} F_n(t) \cos(n\pi/H)z$ in this study, differentiation is easier with respect to z than t.

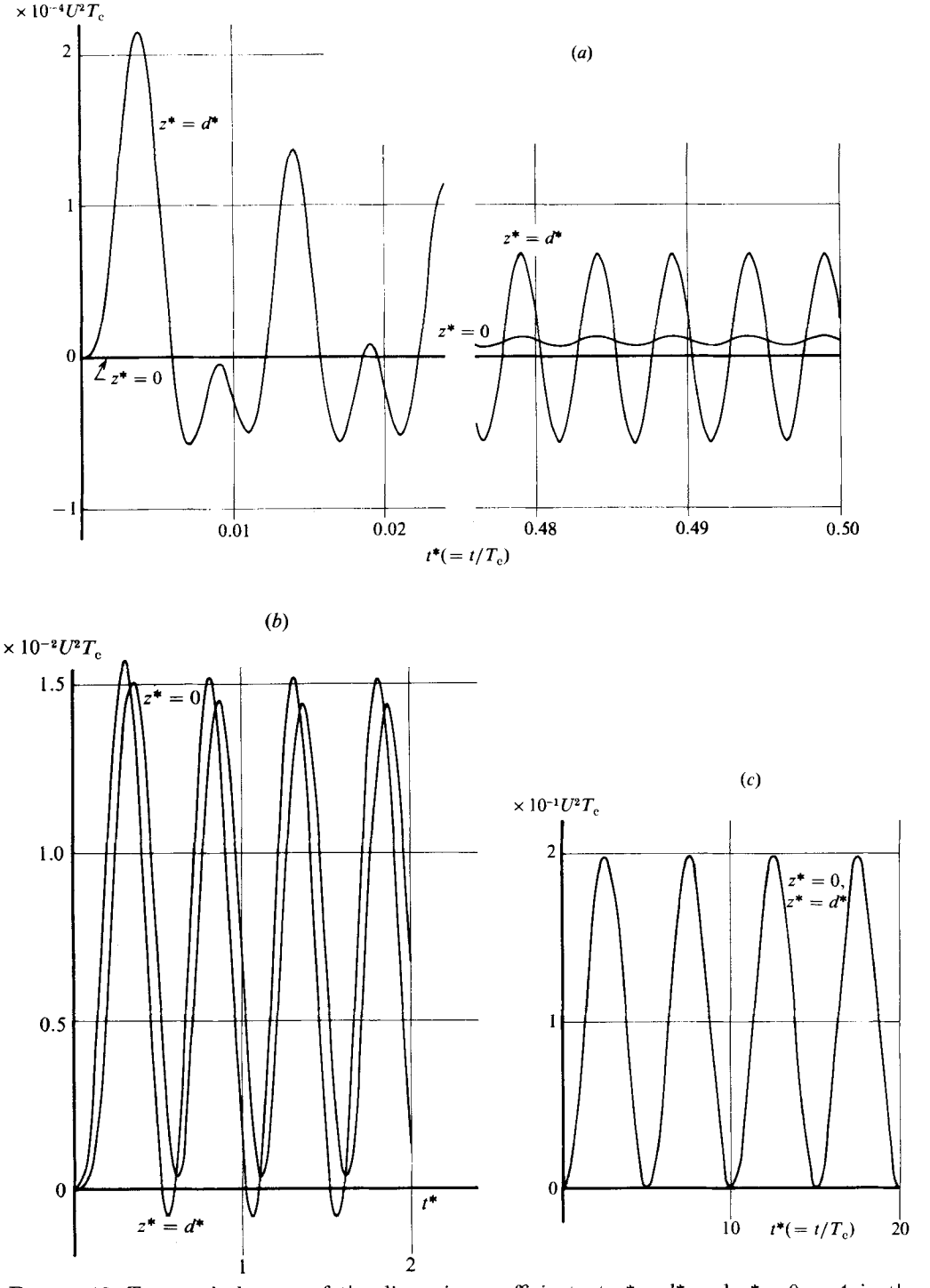

FIGURE 18. Temporal changes of the dispersion coefficient at $z^* = d^*$ and $z^* = 0$ or 1 in the oscillatory current with two-layer flow ($d^* = 0.5$): (*a*) $T_r = 100$; (*b*) 1; (*c*) 0.1.

6. On the negative dispersion coefficient in the oscillatory current

That the vertically averaged dispersion coefficient can be sometimes negative in the oscillatory current was explained in §§3 and 4; this is due to the usual definition of the vertical average. Smith (1983) showed that the increasing rate of the variance (corresponding to the dispersion coefficient) at a particular level can be negative in reversing flows of oscillatory currents. Figure 17(*b*) in the present paper supports the above only during the first tidal period ($0 \leqq t^* \leqq 0.1$). This figure illustrates that the negative dispersion coefficient appears not only in reversing flows but twice for one tidal period at large t. Figure 18 shows the variations of the dispersion coefficients at two particular levels with time in the cases $T_r = 100$, $T_r = 1$ and $T_r = 0.1$. If T_r is very small, it is difficult to detect the negative dispersion coefficient, as was stated by Smith (1983). The negative is by no means for mixing to proceed reversely, i.e. reduction of entropy. It is because the diffusing substance dispersed strongly at a particular level and a certain period is diffused vertically at the following period, which can be seen from figure 16(*b*). The vertically integrated dispersion coefficient (corresponding to $\bar{D}$ in this study if divided by depth); in other words, the dispersion in the two-dimensional (x, z) plane does not become negative, as stated in §4.

7. Concluding remarks

Yasuda (1982) analysed the longitudinal dispersion in an oscillatory current forming a boundary layer given analytically, and studied how the longitudinal dispersion is generated by the shear effect of the oscillatory current. Since it was the primary aim to understand the elementary nature of the longitudinal dispersion in such a current, general characteristics of it could not be sufficiently shown in that paper. The present paper has developed the previous analytical method to deal with longitudinal dispersion due to the shear effect, making a comparison between that in the steady current and that in the oscillatory current. The time-dependence of the vertically averaged dispersion coefficient has been elucidated analytically in both the steady and oscillatory currents, regardless of the vertical profile of the current. The dispersion during the initial stage or its variation within one oscillatory period, which has strong vertical shear of the first-order moment, has required a new definition of the variance and the dispersion coefficient. If we regard the dispersion as a mixing process like turbulent diffusion, the newly defined $\bar{D}$ in this study is considered to be more significant than the usual $\bar{D}^*$ in understanding the dispersion. $\bar{D}$ is by no means negative, even when $\bar{D}^*$ or the dispersion coefficient at a particular level is negative.

The work reported in this paper was carried out as a part of the research conducted at the Government Research Institute, Chugoku, and funded through the Environmental Protection Agency of the Japanese Government.

REFERENCES

Aris, R. 1956 On the dispersion of a solute in a fluid flowing through a tube. *Proc. R. Soc. Lond.* A **235**, 67–77.

Bowden, K. F. 1965 Horizontal mixing in the sea due to a shearing current. *J. Fluid Mech.* **21**, 83–95.

Fischer, H. B., List, E. J., Koh, R. C. Y., Imberger, J. & Brooks, N. H. 1979 *Mixing in Inland and Coastal Waters*. Academic.

HOLLY, E. R., HARLEMAN, D. R. F. & FISCHER, H. B., 1970 Dispersion in homogeneous estuary flow. *J. Hydraul. Div. ASCE* **96**, 1691–1709.

SMITH, R. 1982 Contaminant dispersion in oscillatory flows. *J. Fluid Mech.* **114**, 379–398.

SMITH, R. 1983 The concentration of contaminant distributions in reversing flows. *J. Fluid Mech.* **129**, 137–151.

TAYLOR, G. I. 1953 Dispersion of soluble matter in solvent flowing slowly through a tube. *Proc. R. Soc. Lond.* A **219**, 186–203.

TAYLOR, G. I. 1954 The dispersion of matter in turbulent flow through a pipe. *Proc. R. Soc. Lond.* A **223**, 446–468.

YASUDA, H. 1982 Longitudinal dispersion due to the boundary layer in an oscillatory current – theoretical analysis in the case of an instantaneous line source. *J. Oceanogr. Soc. Japan* **38**, 385–394.